# Anisotropy of light extraction from GaN two-dimensional photonic crystals

**Chun-Feng Lai,[1] Jim-Yong Chi,[2,3*] Hao-Chung Kuo,[1] Chia-Hsin Chao,[3] Han-Tsung Hsueh,[3] Jih-Fu Trevor Wang,[3] and Wen-Yung Yeh[3]**

[1] *Department of Photonics and Institute of Electro-Optical Engineering, National Chiao-Tung University, Hsinchu 300, Taiwan, R.O.C.*
[2] *Institute of Optoelectronic Engineering, National Dong-Hua University, Hualien 97401, Taiwan, R.O.C.*
[3] *Electronics and Opto-electronics Research Laboratories, Industrial Technology Research Institute, Hsinchu 310, Taiwan, R.O.C.*
[*] *Corresponding author: chij@mail.ndhu.edu.tw*

**Abstract:** Angular distribution of light diffracted out of the plane of two-dimensional photonic crystals (PhC) has been studied in the azimuthal direction with a specially designed waveguide structure. The optical images of the light extraction patterns from the guided photoluminescence light are obtained with laser excitation in the center of the annual structure made on GaN multilayer. For increasing lattice constant, symmetric patterns with varying number of petals according to the symmetry of the PhC are observed. The appearance and disappearance of the petals can be explained using the Ewald construction in the reciprocal space. The dependence of light extraction on the lattice constant and orientation, and incident angle are investigated.



**OCIS codes:** (230.5298) Photonic crystals.

## References and links

1. S. Noda, "Recent progresses and future prospects of two- and three-dimensional photonic crystals," IEEE J. Lightwave Technol. **24**, 4554-4567 (2006).
2. F. S. Diana, A. David, I. Meinel, R. Sharma, C. Weisbuch, S. Nakamura, and P. M. Petroff, "Photonic Crystal-assisted light extraction from a Colloidal Quantum Dot/GaN Hybrid Structure," Nano lett. **6**, 1116-1120 (2006).
3. M. Boroditsky, T. F. Krauss, R. Coccioli, R. Vrijen, R. Bhat, and E. Yablonovitch, "Light extraction from optically pumped light-emitting diode by thin-slab photonic crystals," Appl. Phys. Lett. **75**, 1036-1038 (1999).
4. A. Erchak, D. J. Ripin, S. Fan, P. Rakich, and J. D. Joannopoulos, "Enhanced coupling to vertical radiation using a two-dimensional photonic crystal in a semiconductor light-emitting diode," Appl. Phys. Lett. **78**, 563-565 (2001).
5. H. Ichikawa, and T. Baba, "Efficiency enhancement in a light-emitting diode with a two-dimensional surface grating photonic crystal," Appl. Phys. Lett. **84**, 457-459 (2004).
6. A. David, C. Meier, R. Sharma, F. S. Diana, S. P. DenBaars, E. Hu, S. Nakamura, C. Weisbuch, and H. Benisty, "Photonic bands in two-dimensionally patterned multimode GaN waveguides for light extraction," Appl. Phys. Lett. **87**, 101107-1-101107-3 (2005).
7. M. Rattier, H. Benisty, E. Schwoob, C. Weisbuch, T. F. Krauss, C. J. M. Smith, R. Houdré, and U. Oesterle, "Omnidirectional and compact guided light extraction from Archimedean photonic lattices," Appl. Phys. Lett. **83**, 1283-1285 (2003).
8. A. David, T. Fujii, E. Matioli, R. Sharma, K. McGroddy, S. Nakamura, S. P. Denbaars, C. Weisbuch, and H. Benisty, "GaN light-emitting diodes with Archimedean lattice photonic crystals," Appl. Phys. Lett. **88**, 073510-1-073510-3 (2006).
9. C. F. Lai, H. C. Kuo, C. H. Chao, H. T. Hsueh, J.-F. T. Wang, W. Y. Yeh, and J. Y. Chi, "Anisotropy of light extraction from two-dimensional photonic crystal light-emitting diodes," Appl. Phys. Lett. **91**, 123117-1-123117-3 (2007).
10. T. N. Oder, K. H. Kim, J. Y. Lin, and H. X. Jiang, "III-nitride blue and ultraviolet photonic crystal light emitting diodes," Appl. Phys. Lett. **84,** 466-468 (2004).

#91423 - $15.00 USD Received 11 Jan 2008; revised 28 Apr 2008; accepted 28 Apr 2008; published 6 May 2008

11. J. J. Wierer, M. R. Krames, J. E. Epler, N. F. Gardner, and M. G. Craford, "InGaN/GaN quantum-well heterostructure light-emitting diodes employing photonic crystal structures," Appl. Phys. Lett. **84**, 3885-3887 (2004).
12. J. Shakya, K. H. Kim, J. Y. Lin, and H. X. Jiang, "Enhanced light extraction in III-nitride ultraviolet photonic crystal light-emitting diodes," Appl. Phys. Lett. **85**, 142-144 (2004).
13. T. N. Oder, J. Shakya, J. Y. Lin, and H. X. Jiang, "III-nitride photonic crystals," Appl. Phys. Lett. **83**, 1231-1233 (2003).

## 1. Introduction

Nano-sized light scattering objects, arranged periodically in the form the photonic crystal (PhC), provide exciting new ways to manipulate photons. Novel optical properties tunable by the period of the PhC and the size of the nano-objects have been the subject of many research works [1]. The lightwave propagating in the PhC waveguide, with its propagation partially confined by the total internal reflection (TIR), can interact with the reciprocal lattice vectors of the two-dimensional (2D) PhC lattice to exhibit a variety of novel behaviors from the light localization, the super prism effects, and to the negative refraction index behaviors. On the other hand, PhC structure fabricated on light emitting diodes (LEDs) can scatter the guided light into the escaping cone to circumvent the deleterious effects due to TIR which traps the majority of the emitted light in LED chips and converted them to heat [2-13]. In addition, PhC can control the collimating and polarization properties of these escaped lights to offer new possibilities to enhance the performance and to simplify the design of the optical system using LED light sources. For isotropic extraction of light emission, aperiodic PhC patterns have also been reported [6-8], however, for controlling the collimating and polarization properties, periodic PhC with anisotropic light extraction is preferred. Hence a series of paper has been published that utilized a mapping method to describe the angular variation of light extraction intensity in the zenith (vertical) direction [6]. For the azimuthal (in-plane) direction, a direct imaging approach of the in-plane angular distribution of the extracted light from a triangular lattice has also been proposed [9]. In this letter, we report the azimuthal angular distribution of light extraction from square lattices and the comparison with that of the triangular lattice. The observed anisotropy is charted using the Ewald construction according to the lattice constant and the numerical aperture of the observation system. In addition, the polar plots of the light extraction for various PhC lattice orientations are also determined by analyzing the intensity variation with the scanning laser beam. Several novel features particular to the PhC properties have also been directly observed. These results can be used for the optimization of LED devices with PhC extraction.

## 2. Experimental

The PhC structure used for the study is fabricated on the emission surface of a GaN LED structure grown by metal-organic chemical vapor deposition (MOCVD) on c-sapphire substrates. The GaN structure consists of a 1 μm-thick GaN buffer, a 2 μm bottom n-GaN layer, a 100 nm InGaN/GaN multiple quantum wells (MQWs) region, and a 130 nm-thick top p-GaN current spreading layer as shown in Fig. 1(a). The annular region of PhC with an inner/outer diameter of 100/200 μm was patterned by electron-beam (e-beam) lithography. Both triangular and square PhC are patterned for the study. The holes were then etched into the top p-GaN layer using inductively coupled plasma (ICP) dry etching to a depth of 120 nm. The orientation of the PhC is fixed in space and the ratio of hole diameter *d* to lattice constant *a* is also fixed to 0.7 to provide the consistent band structure, as shown in Fig. 1(b).

A micro-photoluminescence (μ-PL) system is utilized in the experiment after fabrication, as shown in Fig. 1(c). A 325 nm He-Cd laser beam normally incidents into the central area of the ring and excites the 470 nm wavelength PL light in the active region. The laser power used is about 3.2 mW and focused to a spot about 5 μm. A 15x UV objective lens with

#91423 - $15.00 USD Received 11 Jan 2008; revised 28 Apr 2008; accepted 28 Apr 2008; published 6 May 2008

numerical aperture (NA) of 0.32 is used to collect the on-axis emission signal from the sample and formed a high-resolution image on a charge-coupled device (CCD) and recorded with a digital camera after filtering out the laser light, as shown inset in Fig. 1(c).

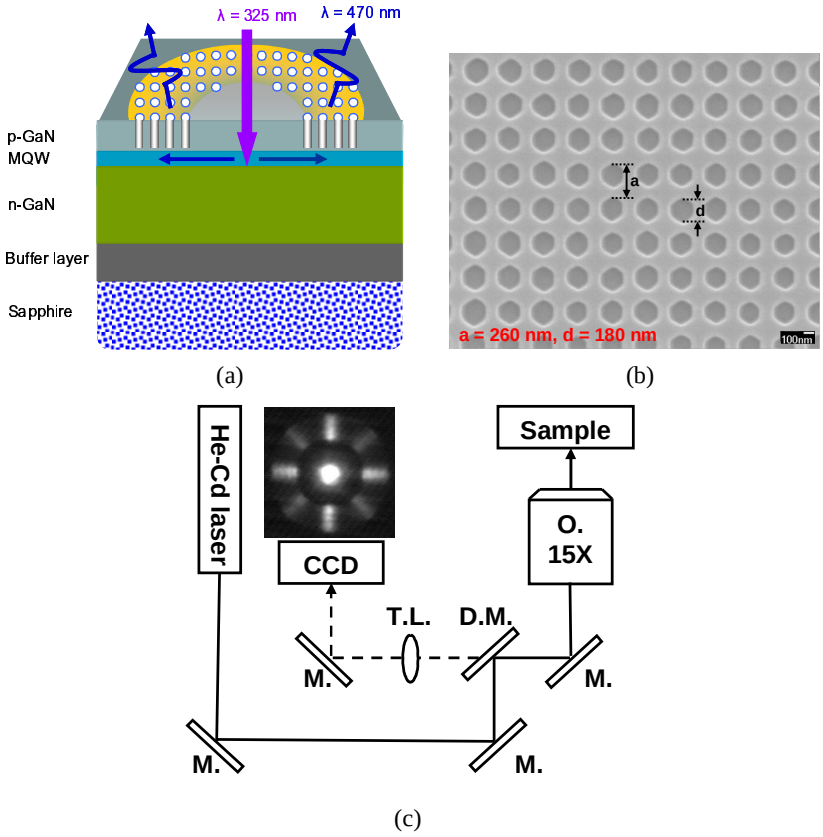


Fig. 1. (a). Schematic diagram of the MOCVD-grown GaN-based blue LED structure (dominant $\lambda$ = 470 nm) with annular PhC region. (b) The top-view scanning electron microscopy (SEM) micrograph of square PhCs on blue LED with the lattice constant $a$ = 260 nm and the diameter of air holes $d$ = 180 nm, and the etch depth $t$ = 120 nm. (c) The μ-PL and CCD imaging system setup, where M.: mirror; T.L.: tube lens; D.M.: dichroic mirror; O.: objective.

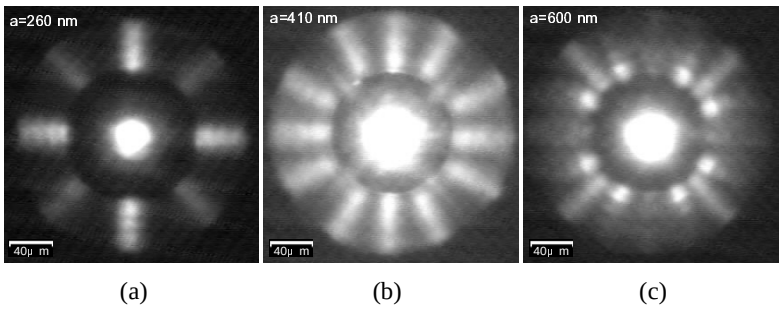


Fig. 2. CCD images taken with square lattices with $a$ = (a) 260 nm, (b) 410 nm, (c) 600 nm. The central bright region in all the photos is due to the unguided PL light excited by the focused laser beam impinging normally in the center.

#91423 - $15.00 USD Received 11 Jan 2008; revised 28 Apr 2008; accepted 28 Apr 2008; published 6 May 2008

## 3. Results and Discussion

Figure 2 depicts the CCD images for the square PhC structures with lattice constants *a* of 260, 410, and 600 nm corresponding to $a/\lambda$ of 0.553, 0.872, and 1.276, respectively. The images are formed by the waveguided 470nm PL light generated by the strongly absorbing 325nm laser light incidents perpendicularly in the center of the structure. After generation, the PL light is partially guided toward the surrounding PhC region by the waveguide formed by the GaN epitaxial layers. This guided light is then coupled into PhC region and diffracted by the PhC lattice while propagating inside the PhC region. Depending on the lattice constant of the PhC, some of the diffracted light left the wafer and formed the images shown in Fig. 2, where the bright region that appeared in the center of all images is due to the unguided PL light. It can be seen that varying number of petals appears as the lattice constant increases. For certain conditions, some of the petals may become weaker or disappeared.

The observed anisotropy may occur at the interface due to the anisotropic coupling when the waveguided PL light enters the PhC region, or in the PhC due to the scattering of the coupled light by the anisotropic crystalline lattice. To estimate the situation for the present case of high $a/\lambda$ and shallow etch, a 3D finite-difference time-domain (FDTD) simulation was carried out to estimate the anisotropy. It shows that the coupling anisotropy decreases when the $a/\lambda$ increases. For the present shallow etch structure and high $a/\lambda$ >0.6, the calculated coupling efficiency is larger than 90% and a variation less than 5% with the incident angles is seen. This indicates that the anisotropic coupling of the PL light at the boundary of the PhC region is relatively weak. The observed anisotropy is, therefore, primarily arisen from the diffraction of guided PL light into air and picked up by the microscope objective.

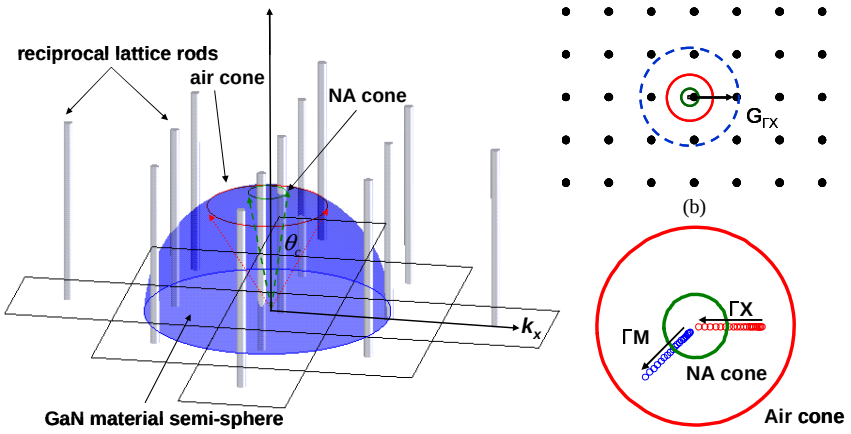


Fig. 3. (a). The Ewald construction for square lattice PhC with *a* = 260 nm. (b) The projection of the Ewald sphere construction on the waveguide plane. (c) The locus of resultant wavevectors for multimode propagation. The direction of the arrows indicates the increasing mode order.

The appearance and disappearance of the petals observed in Fig. 2 can be quantitatively analyzed using the Ewald construction in the reciprocal space. The extraction of waveguiding light into air can be described by the relation $|k + G| < k_0$, where *k* is wavevector of light and *G* is the reciprocal vectors. For extraction into a cone with half angle θ, the relation is $|k + G|/$

#91423 - $15.00 USD Received 11 Jan 2008; revised 28 Apr 2008; accepted 28 Apr 2008; published 6 May 2008

$k_0$< NA, where NA=sin$\theta$ and $\theta$ is the acceptance angle for the observation cone. Such a relation can be represented graphically with the Ewald construction commonly used in the X-ray crystallography. In the present work, for simplicity reason, PhC is treated as a 2D in an overall 3D structure as is commonly done. In such case, the reciprocal lattice of the 2D PhC will be represented as the rods protruding perpendicular to the waveguiding plane. Figure 3(a) depicts the Ewald spheres for a square lattice with the $k$ vector of the incident light pointing directly at a reciprocal lattice point. The center of the sphere is at the end of the vector and the radius is the magnitude of $k$. The intersection points of the sphere with the protruding rods define the extraction direction of the diffracted light. For simplicity, only the in-plane propagation needs to be treated and a consideration of the projection on the waveguiding plane is sufficient. Figure 3(b) shows the projection of the Ewald construction for lattice constant $a$ = 260 nm and $\lambda$ = 470nm. The three circles in the Fig. 3 correspond to 1.) the waveguide mode circle with radius $k = 2n\pi/\lambda$ at the outside, where $n$ is the effective refractive index of the guided wave, 2.) the air disk with radius $k_o = 2\pi/\lambda$ in the middle, and 3.) the NA circle with radius NA=0.32$k_o$ at the inside corresponding to the acceptance angle of the objective lens with NA numerical aperture. When the in-plane component of the resultant wavevector after the coupling to a reciprocal lattice vector falls inside the air circle, the diffracted light can escape into air. However to be picked up with the objective lens, the diffracted light must fall within the NA circle.

For the "thick" waveguides, when the light propagation is multimode, every mode needs to be considered. The in-plane component of each mode after coupling to a particular reciprocal wavevector forms a series of points in the propagation directions. Figure 3(c) illustrates the case for the light propagating in ΓM and ΓX directions in the square lattice shown in Fig. 2(a) with $a$ = 260 nm. Since the thickness of GaN is 3 μm on sapphire, the total number of TE modes is estimated to be 26. The two series of resultant wavevector points after coupling to $G_{\Gamma M}$ and $G_{\Gamma X}$ wavevectors are shown with the arrows indicate the increasing mode order. It can be seen that for the case of image shown in Fig. 2(a), there are 6 higher order modes for ΓX directions that fall in the NA cone and 16 lower order modes in the ΓM directions, yet the intensity of the ΓX pedals appears to be 3 time brighter than that of the ΓX pedals. This observation indicates that the extraction of the higher order modes is more efficient than that of the low order modes and is consistent with the previous report [6].

This simple treatment can be used to explain some of the features in the observed images shown in Fig. 2, considering only the fundamental mode. As shown in Fig. 2(b), for the square lattice with $a$ = 410nm in the ΓM direction, very weak or almost disappearing pedals are seen. The corresponding Ewald constructions for different propagation directions are shown in Fig. 4(b)-(c) with $a$ = 410nm, $\lambda$ = 470 nm, $n$ = 2.17, NA = 0.32 $k_o$. As can be seen that after coupling with the $G_{\Gamma M}$ reciprocal wavevector, no rod fall into the NA circle, but in the other directions, ΓX and ΓXΓM, there is one reciprocal rod for each of them falls in the respective NA circle. Thus one would expect that in the ΓM direction missing diffraction or relatively weak diffraction is observed compared with the other directions. In addition, the predicted angles between $G_{\Gamma X \Gamma M}$ and $G_{\Gamma X}$ or $G_{\Gamma M}$ are 26.6° or 18.4° respectively, in agreement with the observation shown in Fig. 4(a).

A similar case for disappearing petals is observed for the triangular case with $a$ = 600 nm as shown in Fig. 5. The petals along the ΓK directions are missing. The corresponding Ewald construction is shown in Fig. 5(c). As the Ewald sphere for propagation in the ΓK directions, no interception falls inside the NA circle. The Ewald spheres for all the other possible directions are shown in the rest of the Figs. 5(b)-5(f). The angles between the pedals as indicated in Fig. 5(a) are also in agreement with that determined from the involved reciprocal wavevectors.

#91423 - $15.00 USD Received 11 Jan 2008; revised 28 Apr 2008; accepted 28 Apr 2008; published 6 May 2008

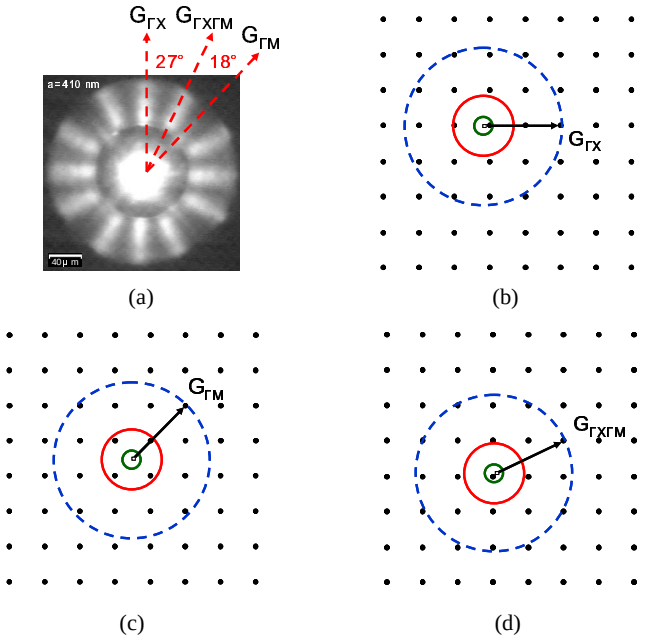


Fig. 4. Reciprocal lattice for square PhC with $a$ = 410nm along the (b) ΓX, (c) ΓM, and (d) ΓXΓM directions with the Ewald spheres explaining the disappearance of the ΓM petals shown in (a).

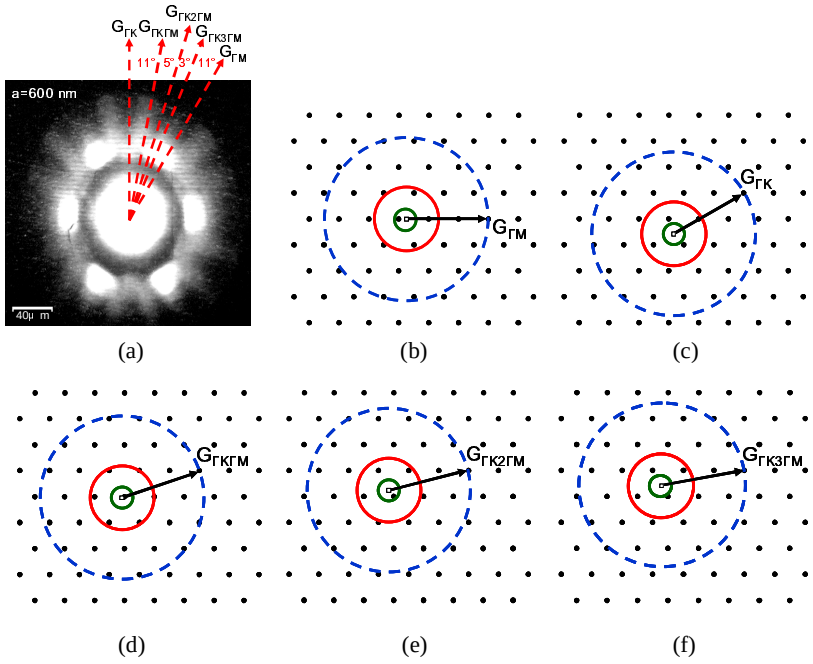


Fig. 5. Reciprocal lattice for triangular lattice PhC with $a$ = 600nm along the (b) ΓM, (c) ΓK, (d) ΓKΓM, (e) ΓK2ΓM, and (f) ΓK3ΓM directions with the Ewald spheres explaining the disappearance of the ΓK petals in (a).

#91423 - $15.00 USD Received 11 Jan 2008; revised 28 Apr 2008; accepted 28 Apr 2008; published 6 May 2008

The above observation established that the use of 2D Ewald construction explains the observed images. It can be invoked to determine the boundaries between regions with varying number of pedals. Following the same procedures for the triangular lattice reported previously [9], a map for the square lattice is shown in Fig. 7. As shown in Fig. 6, as $a/\lambda$ increases above the cutoff, the resultant wavevector will start to couple to the shortest lattice vector $G_{\Gamma X}$. The resultant wavevector falls inside the NA circle (Fig. 6(a)). But for the ΓM direction, the resultant wavevector fall outside the NA circle and will not be seen by the NA=0.32 objective lens (Fig. 6(b)). Therefore, a pattern with 4 petals pointing to ΓX direction is observed. As $a/\lambda$ increases further, the resultant wavevector after coupling to $G_{\Gamma X}$ may fall short of the NA circle and will not be observed (Fig. 6(c)). Thus there is a range of $a/\lambda$ within which the resultant wavevector can fall into the NA circle for a particular propagation direction. The boundary for this range with 4 petals in the ΓX direction start to appear can be determined by the relation $k = |G_{\Gamma X} - \mathrm{NA}|$ to be $a/\lambda = 1/(n+\mathrm{NA})$. For further increase of $a/\lambda$, the resultant wavevector will leave the NA circle as shown Fig. 6(c). In this case $k = |G_{\Gamma X} + \mathrm{NA}|$ and $a/\lambda = 1/(n-\mathrm{NA})$.

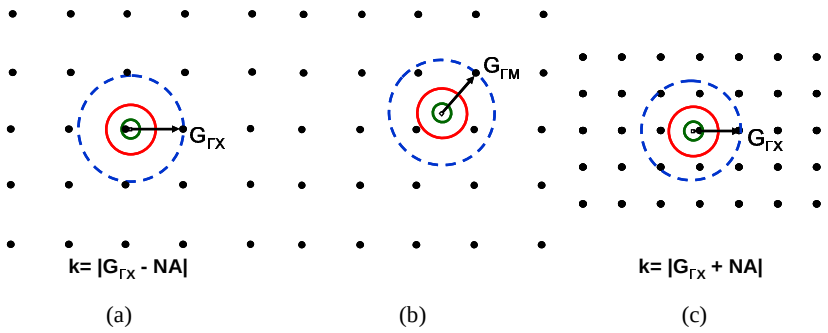


Fig. 6. (a). Reciprocal lattice and Ewald construction for $a/\lambda$ increases above the cutoff and just start to couple with the shortest lattice vector $G_{\Gamma X}$ in the ΓX directions. (b) Shows the situation in the ΓM direction with the resultant wavevector fall outside the NA circle and will not be seen by the NA=0.32 objective. (c) Shows the situation when the $a/\lambda$ increases further to have the $nk_0$ just start to leave the NA circle to disappear from the CCD image.

For larger lattice constants, the escape cone and the guided mode circle become larger relative to the reciprocal lattice. For $a/\lambda > \sqrt{2}/n$, the coupling to $G_{\Gamma M}$ becomes possible and 4 more petals appears representing four equivalent ΓM directions. For even larger lattice constants, coupling to the third nearest wave vectors is possible and the number of petals increases to 16. These increased coupling possibilities are observed as the increased number of petals in the images. The boundaries separating these regions can be readily derived using the Ewald construction as shown in Fig. 7 along with our observations.

The above discussion considers the simple case of single mode propagation in the waveguide plane. Since the thickness of the epitaxial layer used for the present study is 3 μm, the waveguiding is multimode. Every mode can couple with different reciprocal vectors to form their own boundaries for a given number of pedals. When plotted on the map, these boundaries will appear as a band of lines. To clearly present these multimode extraction, only the first and the last mode with mode number '*m*', are shown on Fig. 7. The two outmost lines, $G^{+}_{\Gamma X}$ and $G^{m-}_{\Gamma X}$, define the boundary of the possible $a/\lambda$'s for all the modes that can fall into NA circle after coupling to $G_{\Gamma M}$. The $a/\lambda$ values shown on the right side of Fig. 7 correspond to the boundaries for NA=1.

#91423 - $15.00 USD Received 11 Jan 2008; revised 28 Apr 2008; accepted 28 Apr 2008; published 6 May 2008

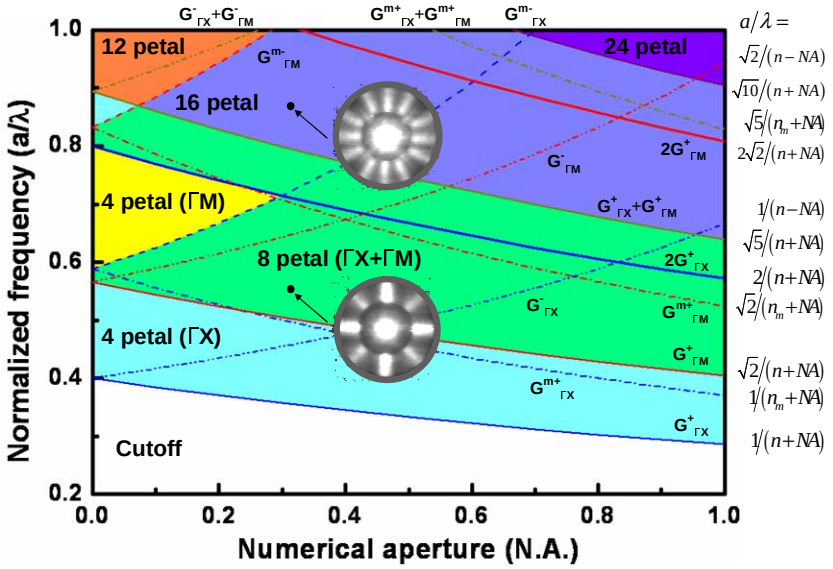


Fig. 7. Map showing regions with different number of petals. The formulas on the right of the figure are the boundary for regions for NA=1. The insets showed the observed 8-fold ($a$ = 260 nm) and 16-fold ($a$ = 410nm) symmetry patterns. The regions of various petals are shown with different colors. The directions of the petals are shown in the parenthesis. The "+" and "-" signs indicate the lower and upper boundary for the regions. The highest mode order number is designated as '$m$' with $n_m$=1.7 (Sapphire) and the maximum index is $n$=2.5 (GaN).

It addition to the case of the normal incidence discussed above, the light extraction for off-normal direction with respect to a particular lattice orientation can also be determined. Such information is important, since many proposed PhC LED structures have separate light generation and extraction regions such that some of the generated light will unavoidably enter the PhC region at off-normal directions. To determine the extraction for the off-normal incidence, the exciting laser beam is scanned along the radius and the CCD images of the extracted light are recorded on different positions along the line, as shown in Fig. 8(a). For a given orientation of the triangular PhC interface, the incident angle can be varied by the scanning laser beam spot as shown in Fig. 8(b) [7]. Thus, the distribution can be determined by taking the intensity from a fixed small area at the interface. The incident angular distribution for the ΓK and ΓM lattice terminations is shown in Fig. 8(c) and 8(d) for $a$=300 nm lattice, respectively. The dashed lines shown in the figures, serving as the visualization aide, are obtained from curve fitting the data points with the Gaussian function. It can be seen that the angular distribution of the extracted light is largely along the ΓM direction no matter what the orientation of the lattice termination even though the waveguiding propagation is isotropic. This observation is consistent with the calculation result described above that coupling into the PhC region is high and the angular variation of the coupling is low.

For the light propagating inside the PhC, the intensity is found to decrease with a decay length of 70-90 μm, depending on the orientation and the holes size. The decay length is determined using the data in the middle dynamic range of the CCD camera where the intensity decay appears as a linear line on the log linear plot. This value is in the same range of that reported in reference 6. Such a parameter is needed for the design of the PhC light extractors.

#91423 - $15.00 USD Received 11 Jan 2008; revised 28 Apr 2008; accepted 28 Apr 2008; published 6 May 2008

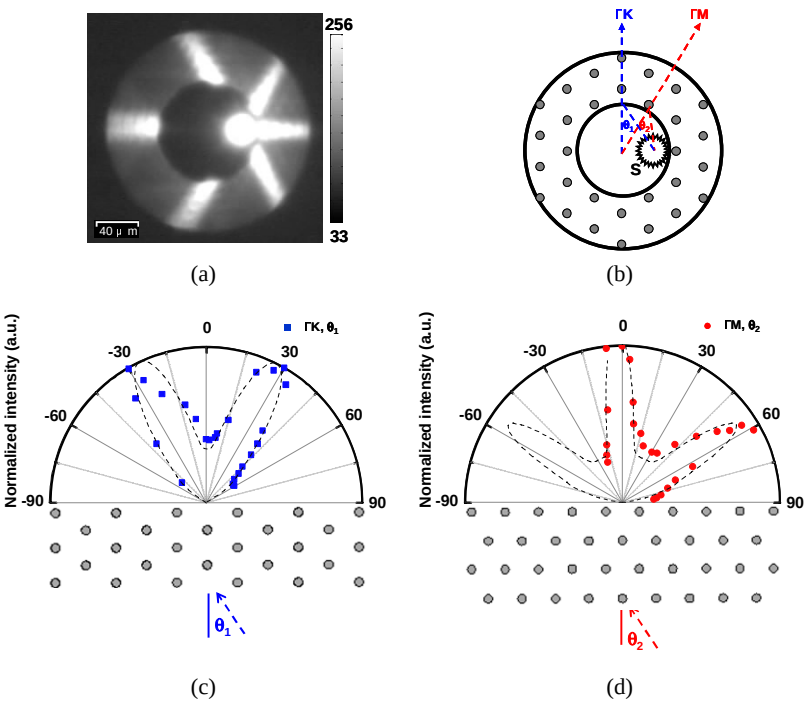


Fig. 8. (a). The observed image when the laser light scanned along the ΓM directions. The intensity scale is shown in the side bar. (b) Schematic shows the incident angles and the normal incident lines for the two directions, where S is the focused laser beam. (c) and (d) show the polar plots of angular dependence of light extraction with the lattice orientation in the (c) ΓK and (d) ΓM directions, respectively.

## 4. Conclusion

In conclusion, we have investigated the anisotropic light extraction dependence on the orientations of the PhC lattice and lattice constants of 2D PhC GaN LED structures. Optical images of the anisotropy in the azimuthal direction are obtained using annular structure with square and triangular lattices. 4- and 6-fold symmetric light extraction patterns are shown with varying number of petals. More petals appear in the observed image with increasing lattice constant, and some of the petals may disappear. The regions for the appearance and disappearance of the petals are determined by the Bragg diffraction analysis using Ewald construction. In addition the angular dependence of the light extraction for waveguided light incidents to plane with various lattice orientations is also determined. The results show that the light extraction for the square and triangular lattices can only occur for certain crystal direction according to the lattice symmetry. The presented imaging approach can also be used to study the propagation of light in the PhC slabs and provides information important for designing LED and other photonic devices to take full advantages of what the photonic crystal can offer.

#91423 - $15.00 USD Received 11 Jan 2008; revised 28 Apr 2008; accepted 28 Apr 2008; published 6 May 2008

**Acknowledgments**

The authors gratefully acknowledge Dr. S. C. Wang at National Chiao-Tung University (NCTU) and Y. S. Liu at National Tsing-Hua University (NTHU) in Taiwan for their technical and management support. This work is supported by the National Nanotechnology Program of Taiwan, R.O.C., and the MOE ATU program and, in part, by the National Science Council of the Republic of China under Contract Nos. NSC 95-2120- M-009-008, NSC 95-2752-E-009-007-PAE, and NSC 95- 2221-E-009-282.

#91423 - $15.00 USD Received 11 Jan 2008; revised 28 Apr 2008; accepted 28 Apr 2008; published 6 May 2008